ELSEVIER

Ceramics International 30 (2004) 1443–1448

CERAMICS
INTERNATIONAL

www.elsevier.com/locate/ceramint

Ternary $Pb(Yb_{1/2}Nb_{1/2})O_3$–$PbZrO_3$–$PbTiO_3$ system as high-T_C/high-piezoelectric materials

W.M. Zhu, Z.-G. Ye*

Department of Chemistry, Simon Fraser University, 8888 University Drive, Burnaby, BC, Canada V5A 1S6

Received 3 December 2003; received in revised form 10 December 2003; accepted 23 December 2003

Abstract

In order to search for high-T_C materials with excellent piezoelectric properties, we have investigated the ternary system of $(1 - x - y)Pb(Yb_{1/2}Nb_{1/2})O_3$–$xPbZrO_3$–$yPbTiO_3$ (PYN–PZ–PT). The phase diagram around the ternary morphotropic phase boundary (MPB) has been determined. For the ceramic of composition near the MPB, $0.33Pb(Yb_{1/2}Nb_{1/2})O_3-0.23PbZrO_3$–$0.44PbTiO_3$, a high ferroelectric Curie temperature of $T_C = 370\,^\circ C$, a very large bipolar strain of 0.4% (peak to peak) at $E = \pm 20\,kV/cm$, a high d_{33} value of 1247 pC/N ($E \leq 20\,kV/cm$) measured from the unipolar dependence of strain, and a remnant polarization (P_r) of 25 $\mu C/cm^3$ are obtained. This performance indicates that this ternary system form promising materials for high-temperature electromechanical transducer applications.

Keywords: B. X-ray methods; C. Piezoelectric properties; Phase transformation; Curie temperature

---

1. Introduction

Relaxor ferroelectrics-based single crystals, namely $(1 - x)Pb(Mg_{1/3}Nb_{2/3})O_3$–$xPbTiO_3$ (PMN–PT), and $(1 - x)Pb(Zn_{1/3}Nb_{2/3})O_3$–$xPbTiO_3$ (PZN–PT), have been intensively investigated in recent years, because of their ultrahigh piezoelectric performance, which may significantly enhance the performance of the piezoelectric devices [1–3]. However, one of the drawbacks of the PMN–PT and PZN–PT single crystals is that their Curie temperatures (T_C) are relatively low, which makes them unsuitable for high-temperature applications. Attempts have been made to develop new systems that can yield materials with both relatively high T_C and high piezoelectricity [4–11]. The $(1 - x - y)Pb(Yb_{1/2}Nb_{1/2})O_3$–$xPbZrO_3$–$yPbTiO_3$ (PYN–PZ–PT) ternary system appears to be a promising candidate. Compositionally ordered $Pb(Yb_{1/2}Nb_{1/2})O_3$ (PYN) is antiferroelectric with a monoclinic perovskite structure and has a T_C around 300 °C [12,13]. It forms a solid solution with $PbTiO_3$, $(1 - x)Pb(Yb_{1/2}Nb_{1/2})O_3$–$xPbTiO_3$ (PYN–PT), with a morphotropic phase boundary (MPB) at $x = 0.46$. The T_C for the MPB composition of this system is around 340 °C [4,6]. $(1 - x)PbZrO_3$–$xPbTiO_3$ (PZT) is a well-known binary system which shows good piezoelectricity and high T_C (370 °C) at the MPB composition ($x \sim 0.47$) [14]. However, single crystals of PZT are very difficult to grow due to the high melting point of PZ [15]. It is reasonable to expect that an MPB could form for the PYN–PZ–PT ternary system and the piezoelectricity and T_C of the MPB composition would be high because of the similar perovskite structures for the three end members and the high T_C for both PYN–PT and PZT at the MPB compositions. Indeed, the ternary MPB was confirmed in a number of recent papers [16–19]. However, there is inconsistency among the MPB compositions reported by different researchers, and the piezoelectric properties measured were not as good as expected. Therefore, in this work we have systematically investigated the MPB compositions of the PYN–PZ–PT system. The ternary phase diagram around the MPB has been completed and the bipolar and unipolar strains of the MPB ceramics characterized.

2. Experimental

Ceramic samples of the $(1 - x - y)$PYN–xPZ–yPT, with $x = 0.1$, $y = 0.4$–0.5; $x = 0.23$, $y = 0.29$–0.38; $x = 0.35$, $y = 0.28$–0.47; and $x = 0.47$, $y = 0.34$–0.48, were

---

[*] Corresponding author. Tel.: +1-604-291-3351; fax: +1-604-291-3765.
E-mail address: zye@sfu.ca (Z.-G. Ye).

0272-8842/$30.00 © 2004 Elsevier Ltd and Techna Group S.r.l. All rights reserved.
doi:10.1016/j.ceramint.2003.12.071

prepared by the "columbite" method [20] in order to prevent the formation of an undesired pyrochlore phase. Yb_2O_3 (99.9%) and Nb_2O_5 (99.9%) were mixed and calcined at 1100 °C for 4 h at first, and then mixed with stoichiometric PbO (99.9%), ZrO_2 (99%) and TiO_2 (99.9%), to be calcined at 850 °C for 2 h. After grinding for 3 h with 5% polyvinyl alcohol binder, the calcined powders were pressed into pellets, which were heated at 700 °C for 1 h to eliminate the binder, and then buried in calcined powders of the same composition for sintering. The sintering took place in a sealed Al_2O_3 crucible at 1220 °C for 2 h, After sintering, the surfaces of the ceramics were polished and sputtered with gold layers as electrodes for electric characterization. The phases of the calcined powders and sintered ceramics were identified and analyzed using a Philips PW 1730 diffractometer with a Cu Kα source. The dielectric properties were measured by a Solartron 1260 Impedance Analyzer combined with a Solartron 1296 Dielectric Interface. The dielectric hysteresis measurements were carried out on a RT-66A (Radiant Technologies) Standard Testing System using the "Virtual Ground" mode at a frequency of 10 Hz. The unipolar and bipolar strains for the ceramics were measured by an MTI-2000 photonic sensor. For the unipolar strain measurement, the samples were poled in silicone oil at 160 °C at an electrical field of 25 kV/cm which was kept for 10 min.

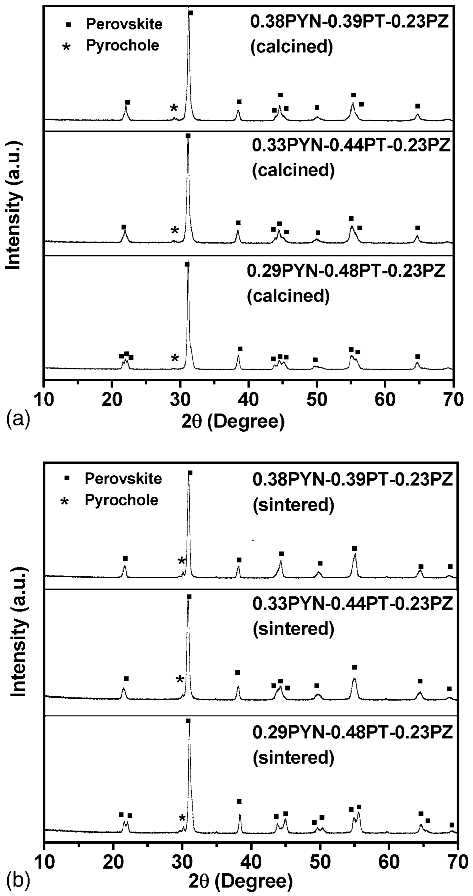

Fig. 1. XRD spectra for the 0.38PYN–0.23PZ–0.39PT, 0.33PYN–0.23PZ–0.44PT and 0.29PYN–0.23PZ–0.48PT ceramics after calcination (a) and sintering (b).

3. Results and discussion

3.1. Ternary morphotropic phase boundary

In order to determine more accurately the MPB of the ternary system, powder X-ray diffraction (XRD) was performed on all the compounds synthesized, and the phase components were carefully analyzed. Taking $x = 0.23$ series as an example, the XRD patterns (Fig. 1) show a majority of the perovskite phase with only a trace amount of the pyrochlore phase for both calcined and sintered samples. The amount of pyrochlore phase decreases with the decrease of PYN component in the composition (Fig. 1a). The phase analysis was performed on the XRD patterns from $2\theta = 43$–$46°$, where the tetragonal phase shows two peaks T(0 0 2) and T(2 0 0), while the rhombohedral phase shows only one peak R(2 0 0). The XRD profiles in this region were deconvoluted with the Gaussian functions, and the ratio of tetragonal to rhombehedral phase was determined by the term: $\mathrm{T/R} = [I_{\mathrm{T}(002)} + I_{\mathrm{T}(200)}]/I_{\mathrm{R}(200)}$, where $I_{\mathrm{R}(200)}$ represents the area of the deconvoluted R(2 0 0) peak, and $I_{\mathrm{T}(002)}$ and $I_{\mathrm{T}(200)}$, the areas of the tetragonal (0 0 2) and (2 0 0) peaks, respectively. Fig. 2 shows that, for each series, there is a broad region where two phases, rhombohedral and tetragonal, coexist, indicating the typical morphotropic phase behaviour. The phase ratio (T/R) increases with the increase of y (PT), so that there is a composition, in each series of x, at which the phase ratio is close to 1. This composition is chosen as one of the morphotropic phase boundary compositions. For the compositions studied here, those close to the MPB are found to be: 0.48PYN–0.10PZ–0.42PT, 0.38PYN–0.23PZ–0.39PT, 0.24PYN–0.35PZ–0.41PT and 0.11PYN–0.47PZ–0.42PT. These points, together with the previously reported MPB compositions for PZT [14] and PYN–PT [4], have allowed us to establish a morphotropic phase boundary in this ternary phase diagram, as shown in Fig. 3.

The compounds of the $x = 0.23$ series were then sintered and processed to form ceramics for dielectric and piezoelectric characterization. After sintering, the amount of pyrochlore phase in each sample is found to increase slightly, probably due to the evaporation of PbO during sintering process. At the same time, the phase ratio (T/R) of the sintered samples changes from that of the calcined samples for the same starting composition (Fig. 1). For the calcined samples, all 3 compositions of this series show the coexistence of the rhombohedral and tetragonal phases (Fig. 1a). For the sintered samples, however, 0.38PYN–0.23PZ–0.39PT is rhombohedral, 0.29PYN–0.23PZ–0.48PT is tetragonal, and only 0.33PYN–0.23PZ–0.44PT shows the coexistence of two phases with $\mathrm{T/R} = 1.22$ (Fig. 4). This is evidenced from the single peak for 0.38PYN–0.23PZ–0.39PT, the

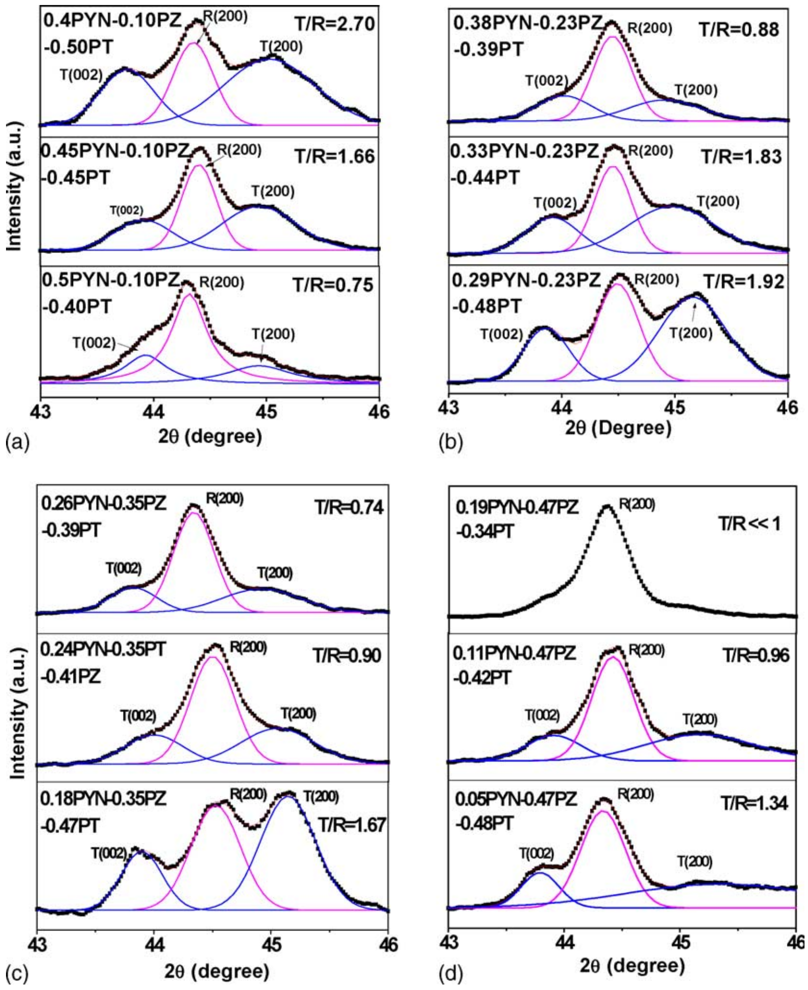

Fig. 2. Phase ratios of the calcined $(1-x-y)$PYN–xPZ–yPT compounds for the composition series of $x = 0.1$ (a), $x = 0.23$ (b), $x = 0.35$ (c) and $x = 0.47$ (d).

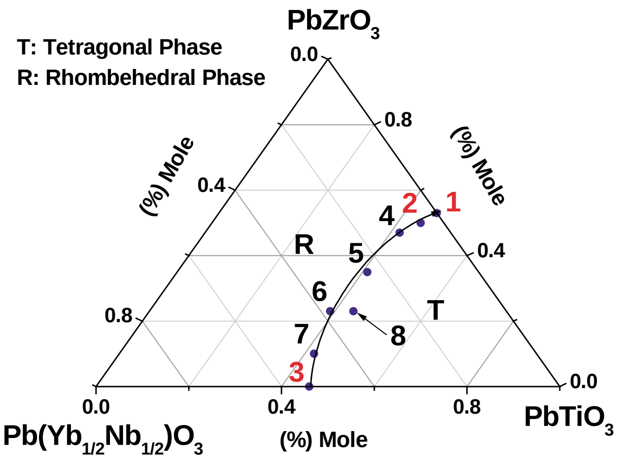

Fig. 3. MPB phase diagram for $(1-x)$PYN–xPZ–yPT ternary system. Points 4, 5, 6, 7, 8 are from this work, Point 1 from Ref. 14, Point 2 from Ref. 16, and Point 3 from Ref. 4. The composition of Point 8 is 0.33PYN–0.23PZ–0.44PZ.

dublet split for 0.29PYN–0.23PZ–0.48PT and the triplet split for 0.33PYN–0.23PZ–0.44PT from the cubic (2 0 0) reflection at 2θ around 45° (Fig. 1b). This result indicates that the width of the composition region for the two-phase coexistence decreases in ceramics after sintering which have large grains. This observation is consistent with the

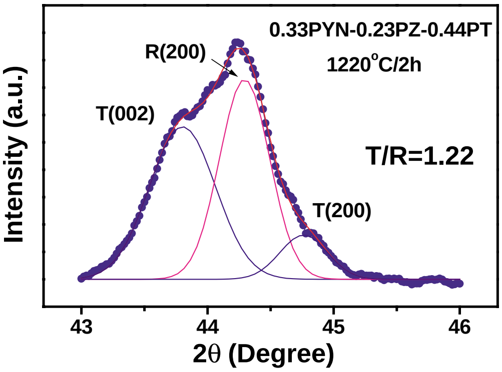

Fig. 4. Phase components of the 0.33PYN–0.23PZ–0.44PT ceramic after sintering.

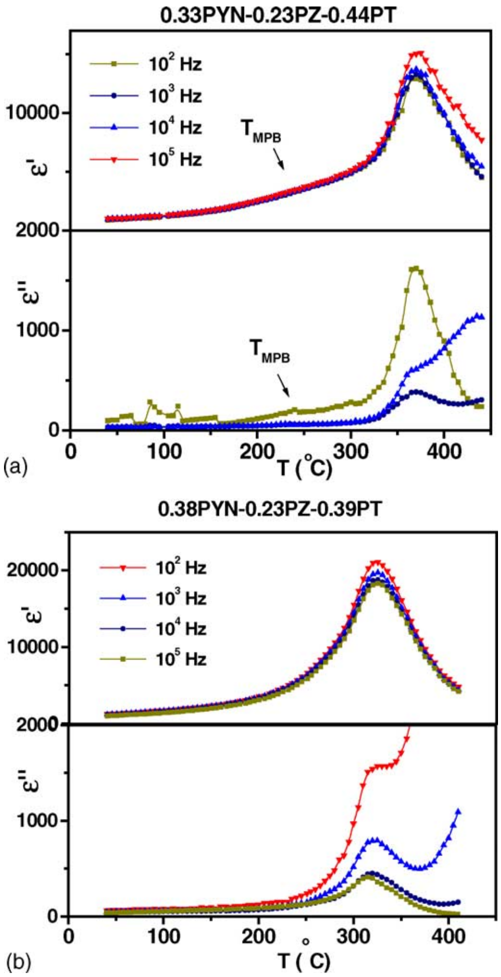

Fig. 5. Temperature variation of the real (ε') and imaginary (ε'') parts of dielectric permittivity for (a) 0.33PYN–0.23PZ–0.44PT and (b) 0.38PYN–0.23PZ–0.39PT ceramics measured at different frequencies.

inference from the probability polyhedron model developed by Cao and Cross [21], which states that at the MPB, the larger the grain size, the narrower the region of composition for two-phase coexistence. In this work, for the $x = 0.23$ series, the composition that is close to the MPB changes from 0.38PYN–0.23PZ–0.39PT after calcination to 0.33PYN–0.23PZ–0.44PT after sintering.

3.2. Dielectric and ferroelectric properties

Fig. 5 shows the temperature dependences of the real (ε') and imaginary (ε'') parts of dielectric permittivity measured at 10^2–10^5 Hz for 0.33PYN–0.23PZ–0.44PT and 0.38PYN–0.23PZ–0.39PT ceramics. The temperature dependence of ε' for both samples shows a broad peak at T_C which does not depend on frequency. T_C is 325 °C for 0.38PYN–0.23PZ–0.39PT ceramic and 370 °C for 0.33PYN–0.23PZ–0.44PT ceramic. Apart from T_C, a change in slope is found at around 235 °C for 0.33PYN–0.23PZ–0.44PT, which seems to indicate a rhombohedral/tetragonal transition, T_{MPB} (or T_{RT}), as observed in the MPB compositions of PMN–PT system between 80 and 100 °C, The phase transitions at T_C and T_{MPB} are also observed on the imaginary part of dielectric permittivity (ε'') (with some fluctuations at low temperature) (Fig. 5). Therefore the ceramic of 0.33PYN–0.23PZ–0.44PT exhibits not only a higher T_C but also a higher T_{MPB} than the PMN–PT and PZN–PT systems. No anomaly other than T_C is found for 0.38PYN–0.23PZ–0.39PT. At room temperature, both samples show a fairly high ε' (997 for 0.38PYN–0.23PZ–0.39PT and 991 for 0.33PYN–0.23PZ–0.44PT) and low dielectric dissipation factor ($\tan\delta = 0.04$ for 0.38PYN–0.23PZ–0.39PT and 0.02 for 0.33PYN–0.23PZ–0.44PT) with almost no frequency dispersion.

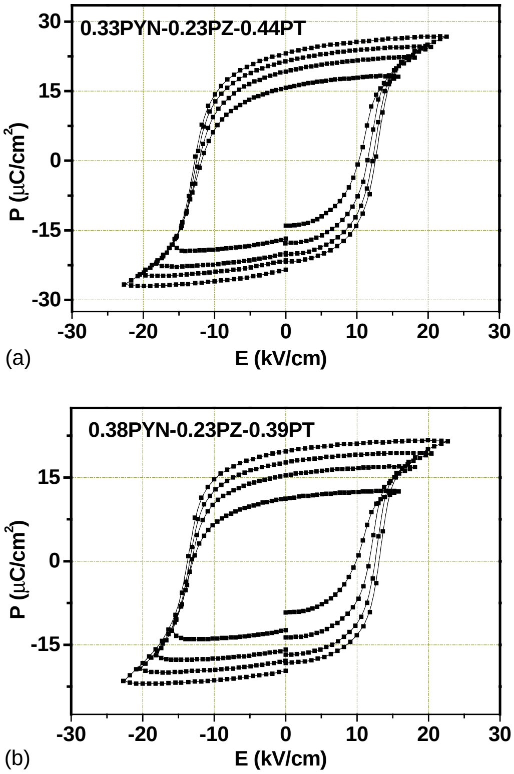

Fig. 6. Dielectric hysteresis loops for the 0.33PYN–0.23PZ–0.44PT and 0.38PYN–0.23PZ–0.39PT ceramics measured at various field strengths.

Fig. 6 gives the dielectric hysteresis loops for the two ceramics. Both samples exhibit well-defined square-like loops with saturation at an electric field of ±23 kV/cm. The remnant polarization P_r is 20 μC/cm² for 0.38PYN–0.23PZ–0.39PT, and 25 μC/cm² for 0.33PYN–0.23PZ–0.44PT.

3.3. Piezoelectric properties

Unipolar and bipolar strains were measured under the application of an electrical field up to 20 and ±20 kV/cm, respectively. For unipolar strain (Fig. 7), apart from small fluctuations for the two curves and small hysteresis for the curve of 0.33PYN–0.23PZ–0.44PT ceramic, the variation of the unipolar strain with electric field for both samples are basically linear, the slopes of which are used to calculate

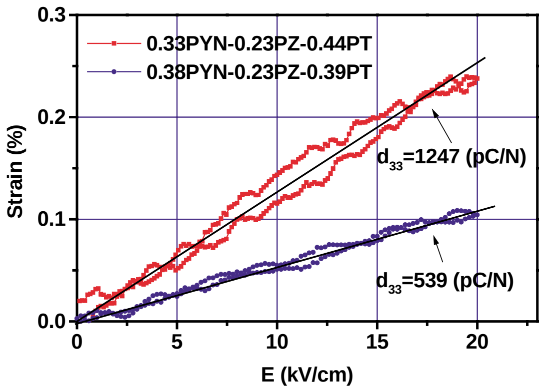

Fig. 7. Unipolar strain for the 0.33PYN–0.23PZ–0.44PT and 0.38PYN–0.23PZ–0.39PT ceramics.

the piezoelectric coefficient d_{33}. The d_{33} value is found to be 539 pC/N for the 0.38PYN–0.23PZ–0.39PT ceramic and 1247 pC/N for the 0.33PYN–0.23PZ–0.44PT ceramic. The latter shows a very good piezoelectric property. Taking into consideration the relatively high T_C (370 °C) for 0.33PYN–0.23PZ–0.44PT, this material is undoubtedly a promising candidate for high temperature high performance piezoelectric applications.

In consistence with the large unipolar strain, a large bipolar strain (0.4% peak to peak) was also found for the 0.33PYN–0.23PZ–0.44PT ceramic, while the bipolar strain for the 0.38PYN–0.23PZ–0.39PT ceramic is comparatively smaller (0.09% peak to peak) (Fig. 8). Since the bipolar strain has significant contribution from domain reverse [22], the large bipolar strain for the 0.33PYN–0.23PZ–0.44PT ceramic suggests an enhanced piezoelectric effect due to the ease of multi-domains reversal and polarization switching arising from the coexistence of the rhombohedral and tetragonal phases around the MPB. The unipolar strains exhibit rather a linear variation without significant change of slope. This indicates that the unipolar strain mainly results from the inverse piezoelectric effect within the electric field region for measurement ($E \leq 20$ kV/cm), which is lower than the poling field.

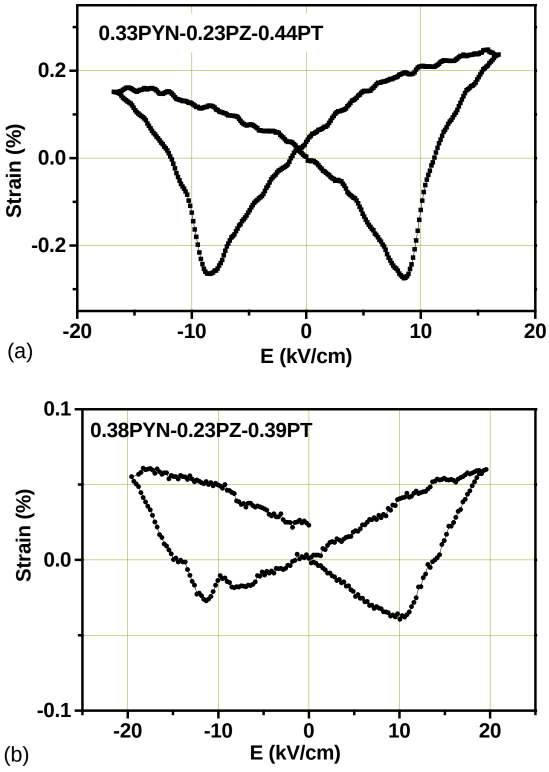

Fig. 8. Bipolar strain for the 0.33PYN–0.23PZ–0.44PT and 0.38PYN–0.23PZ–0.39PT ceramics.

4. Conclusions

The ceramics of the $(1-x-y)\mathrm{Pb(Yb_{1/2}Nb_{1/2})}$–$x\mathrm{PbZrO_3}$–$y\mathrm{PbTiO_3}$ ternary system with perovskite structure have been synthesized by solid state reactions. The partial ternary phase diagram near the MPB has been determined by phase analysis of the XRD patterns from calcined samples. The compositions of the ternary MPB are found to be 0.48PYN–0.10PZ–0.42PT, 0.38PYN–0.23PZ–0.39PT, 0.24PYN–0.35PZ–0.41PT and 0.11PYN–0.47PZ–0.42PT with the tetragonal over rhombohedral phase ratio close to 1. The two-phase coexistence region in this system narrows after sintering at 1220 °C, and the phase ratio (T/R) changes slightly for the compositions with two-phase coexistence around MPB. The 0.33PYN–0.23PZ–0.44PT ceramic with a phase ratio (T/R) close to 1 after sintering shows excellent piezoelectric properties with a $d_{33} = 1247$ pC/N, a high T_C (370 °C), a high T_{MPB} (235 °C) and a large bipolar strain (0.4% peak to peak) at an electric field of ±20 kV/cm. Well-saturated dielectric hysteresis loops were displayed at $E = \pm 23$ kV/cm with $P_r = 25\ \mu\mathrm{C/cm^2}$ for 0.33PYN–0.23PZ–0.44PT ceramic, indicating good ferroelectric properties. The excellent piezoelectric and ferroelectric properties of this material make it a promising candidate for high temperature high piezoelectric applications.

Acknowledgements

This work was supported by the US Office of Naval Research (Grant No. N00014-99-1-0378).

References

[1] S.-E. Park, T.R. Shrout, Ultrahigh strain and piezoelectric behavior in relaxor based ferroelectric single crystals, J. Appl. Phys. 82 (4) (1997) 1804.
[2] Z.-G. Ye, Crystal chemistry and domain structure of relaxor piezocrystals, Curr. Opin. Solid State Mater. Sci. 6 (2002) 35.
[3] S.-E. Park, W. Hackenberger, High performance single crystal piezoelectrics: applications and issues, Curr. Opin. Solid State Mater. Sci. 6 (2002) 11.

[4] S.J. Zhang, S. Rhee, C.A. Randall, T.R. Shrout, Dielectric and piezoelectric properties of high Curie temperature single crystals in the $Pb(Yb_{1/2}Nb_{1/2})O_3$–$x$$PbTiO_3$ solid solution series, Jpn. J. Appl. Phys. 41 (2002) 722.

[5] S.J. Zhang, P.W. Rehrig, C. Randall, T.R. Shrout, Crystal growth and electrical properties of $Pb(Yb_{1/2}Nb_{1/2})O_3$–$PbTiO_3$ perovskite single crystals, J. Cryst. Growth 234 (2002) 415.

[6] T. Yamamoto, S. Ohashi, Dielectric and piezoelectric properties of $Pb(Yb_{1/2}Nb_{1/2})O_3$–$PbTiO_3$ solid solution system, Jpn. J. Appl. Phys. 34 (1995) 5349.

[7] R.E. Eitel, C.A. Randall, T.R. Shrout, P.W. Rehrig, W. Hackenberger, S.-E. Park, New high temperature morphotropic phase boundary piezoelectrics based on $Bi(Me)O_3$–$PbTiO_3$ ceramics, Jpn. J. Appl. Phys. 40 (2001) 5999.

[8] R.E. Eitel, C.A. Randall, T.R. Shrout, S.-E. Park, Preparation and characterization of high temperature perovskite ferroelectrics in the solid-solution $(1-x)BiScO_3$–$x$$PbTiO_3$, Jpn. J. Appl. Phys. 41 (2002) 2099.

[9] T.-H. Song, R.E. Eitel, T.R. Shrout, C.A. Randall, W. Hackenberger, Piezoelectric properties in the perovskite $BiScO_3$–$PbTiO_3$–(Ba, Sr)TiO_3 ternary system, Jpn. J. Appl. Phys. 42 (2003) 5181.

[10] N. Yasuda, H. Ohwa, M. Kume, Y. Yamashita, Piezoelectric properties of a high curie temperature $Pb(In_{1/2}Nb_{1/2})O_3$–$PbTiO_3$ binary system single crystal near a morphotropic phase boundary, Jpn. J. Appl. Phys. 39 (2000) L66.

[11] Y. Hosono, Y. Yamashita, H. Sakamoto, N. Ichinose, Dielectric and piezoelectric properties of $Pb(In_{1/2}Nb_{1/2})O_3$–$Pb(Mg_{1/3}Nb_{2/3})O_3$–$PbTiO_3$ ternary ceramic materials near the morphotropic phase boundary, Jpn. J. Appl. Phys. 42 (2003) 535.

[12] J.R. Kwon, W.K. Choo, The antiferroelectric crystal structure of the highly ordered complex perovskite $Pb(Yb_{1/2}Nb_{1/2})O_3$, J. Phys.: Condens. Matter 3 (1991) 2147.

[13] Y.Y. Tomashpolskii, Y.N. Venevtsev, X-ray and electrical investigations of the system $PbCo_{1/2}W_{1/2}O_3$–$PbYb_{1/2}Nb_{1/2}O_3$, Sov. Phys. Solid State (English Transl.) 6 (1965) 2388.

[14] B. Jaffe, W.R. Cook, H. Jaffe, Piezoelectric Ceramics, Academic Press, London, 1971.

[15] S. Fushimi, T. Ikeda, Phase equilibrium in the system PbO–TiO_2–ZrO_2, J. Am. Ceram. Soc. 50 (1967) 129.

[16] K.V Im, W.K. Choo, Dielectric properties and phase transition of $0.5[(1-x)Pb(Yb_{1/2}Nb_{1/2})O_3$–$x$$PbTiO_3]$–$0.5PbZrO_3$ solid solution, Jpn. J. Appl. Phys. 36 (1997) 5989.

[17] K.H. Yoon, H.K. Lee, H.R. Lee, Electrical mechanical properties of $Pb(Yb_{1/2}Nb_{1/2})O_3$–$PbZrO_3$–$PbTiO_3$, J. Am. Ceram. Soc. 85 (11) (2002) 2753.

[18] H. Ohuchi, S. Tsukamoto, M. Ishii, H. Hayakawa, Piezoelectric and structure properties of $Pb(Yb_{1/2}Nb_{1/2})O_3$–$PbTiO_3$–$PbZrO_3$ ceramics, J. Eur. Ceram. Soc. 19 (1999) 1191.

[19] K.H. Yoon, Y.S. Lee, H.R. Lee, Effect of $Pb(Yb_{1/2}Nb_{1/2})O_3$ on structural and piezoelectric properties of $Pb(Zr_{0.52}Ti_{0.48})O_3$ ceramics, J. Appl. Phys. 88 (6) (2000) 3596.

[20] S.L. Swartz, T.R. Shrout, Fabrication of perovskite lead magnesium niobate, Mater. Res. Bull. 17 (1982) 1245.

[21] W. Cao, L.E. Cross, Theoretical model for the morphotropic phase boundary in lead zirconate–lead titanate solid solution, Phys. Rev. B 47 (9) (1993) 4825.

[22] D. Damjanovic, Ferroelectric, dielectric and piezoelectric properties of ferroelectric thin films and ceramics, Rep. Prog. Phys. 61 (1998) 1267.